Airborne Laser Infrared Absorption Spectrometer (ALIAS-II) for *In situ* Atmospheric Measurements of N_2O, CH_4, CO, HCl, and NO_2 from Balloon or RPA Platforms

David C. Scott, Robert L. Herman, Christopher R. Webster, Randy D. May

Gregory J. Flesch, and Elisabeth J. Moyer

Jet Propulsion Laboratory

California Institute of Technology

4800 Oak Grove Drive

Pasadena, CA 91109

The Airborne Laser Infrared Absorption Spectrometer II (ALIAS-II) is a lightweight, high-resolution (0.0003 cm^{-1}), scanning, mid-infrared absorption spectrometer based on cooled (80 K) lead-salt tunable diode laser sources. It is designed to make *in situ* measurements in the lower and middle stratosphere on either a balloon platform or high-altitude remotely piloted aircraft (RPA). Chemical species that can be measured precisely include long-lived tracers N_2O, CH_4, the shorter-lived tracer CO, and chemically active species HCl and NO_2. Advances in electronic instrumentation developed for ALIAS-I, with the experience of more than 250 flights on board NASA's ER-2 aircraft, have been implemented in ALIAS-II. The spectrometer is a two-channel spectrometer with an open cradle, multipass absorption cell to ensure minimal contamination from inlet and surfaces. Time-resolution of the instrument is ≤ 3 seconds, allowing rapid *in situ* measurements with excellent spatial resolution. ALIAS-II has completed seven successful balloon flights from New Mexico, Alaska, and Brazil providing CH_4 and N_2O vertical profiles in the tropics, mid-, and high- northern latitudes up to altitudes of 32 km.

010 1280

1. INTRODUCTION

ALIAS-II is a dual-channel scanning laser spectrometer designed to make simultaneous *in situ* measurements of various combinations of the gases N_2O, CH_4, CO, HCl, and NO_2 to altitudes above 30 km on a balloon gondola or high-altitude remotely piloted aircraft (RPA). This instrument complements existing scientific platforms used to study stratospheric chemistry. Unlike existing instruments on high-altitude aircraft such as NASA's ER-2 or DC-8, ALIAS-II directly probes the middle stratosphere at altitudes above 21 km, where ozone photochemistry is most active. In addition, ALIAS-II has demonstrated high accuracy during seven balloon flights. Previous balloon measurements of N_2O and CH_4 in the tropics[1,2] have estimated uncertainties of 10% to 25%, and satellite N_2O data from the Cryogenic Limb Array Etalon Spectrometer (CLAES)[3] have roughly 20% uncertainty.[4] Other remote sensing instruments, such as the Atmospheric Trace Molecule Spectroscopy (ATMOS) spectrometer, have precision better than 5% for stratospheric N_2O and CH_4,[5] but limited spatial resolution. In contrast ALIAS-II has an excellent vertical resolution of 15 meters, unattainable by any remote-sensing instrument.

The scientific rationale for building this instrument is the need for highly accurate measurements of trace gases in the middle stratosphere, especially in the tropics, where *in situ* measurements are very limited.[1,2] The first scientific study using ALIAS-II was an analysis of stratospheric dynamics using measurements of the long-lived tracers N_2O and CH_4 obtained during five balloon flights in the tropics, mid-latitudes, and high latitudes.[6] This study constrained stratospheric mixing time scales, which are an essential input into assessment models of the stratospheric effects of the proposed high-speed civil transport (HSCT) fleet.[7,8] HSCTs inject nitrogen oxides (NO_x) directly into the lower stratosphere,

where NO_x catalytically destroys O_3.[9,10] At lower altitudes, NO_x acts as a catalyst to produce O_3 in reactions involving the oxidation of methane and other hydrocarbons.[11] The proposed fleets of HSCTs will also inject large amounts of CO_2 and H_2O into the atmosphere, which could also have a profound effect on the climate.[12] Observations of tracer profiles at different latitudes and seasons are an essential element of investigations of the transport of aircraft emissions and, more generally, stratospheric air parcels.[6,13]

Simultaneous measurements of tracers with different lifetimes in the stratosphere can lead to valuable insight into dynamical transport phenomenon. The balloon support facility of the Jet Propulsion Laboratory designed and built a lightweight gondola capable of carrying multiple instruments above 30 km. For the Stratospheric Tracers of Atmospheric Transport (STRAT), Observations from the Middle Stratosphere (OMS), and Photochemistry of Ozone Loss in the Arctic Region In Summer (POLARIS) campaigns of 1996-98 the payload consisted of ALIAS-II, a nondispersive infrared CO_2 analyzer (Harvard),[14] a Lightweight Airborne Chromatograph Experiment (LACE),[15] an Ozone UV photometer (JPL),[16] a frost point hygrometer (NOAA H_2O),[17] and another laser infrared spectrometer (Argus).[18] These 6 instruments produce data sets that extend well into the middle stratosphere and allow analysis of the age and origins of the air parcels sampled.[19]

ALIAS-II has successfully retrieved *in situ* vertical profiles of the two long-lived tracers N_2O and CH_4 between 6 km and 32 km on the JPL OMS platform as part of NASA's STRAT, OMS, and POLARIS campaigns. ALIAS-II and the OMS payload are lightweight and compact to allow great flexibility in deployments to a large number of launch sites ranging from the Arctic to the tropics. Tropical measurements of multiple tracers are especially important because there is a lack of simultaneous *in situ* data above

21 km. The excellent spatial resolution of the instrument (15-meter vertical resolution during balloon descent) allows a determination of the spatial scales that are most important to stratospheric transport. Vertical resolution of the instrument is determined by the ascent or descent rate and the time required to exchange the air in the Herriott cell. During the flights from Ft. Sumner, New Mexico in 1996, the mean descent rate was 140 m/min (range = 30-270 m/min), rapid enough to ensure that the air sampled in the Herriott cell is completely replaced before each integration period. To make full use of the data from ALIAS-II, the N_2O and CH_4 profiles are intercompared with model results, ER-2 data up to 21 km, satellite observations (UARS HALOE),[20] and other remote-sensing instruments such as ATMOS[21,22,5] on the space shuttle, as well as JPL's Submillimeter Limb Sounder (SLS),[23] and Mark IV.[24]

In addition to N_2O and CH_4, ALIAS-II will supply *in situ* measurements of the chemically active species[25,26] HCl, NO_2 and the tracer CO. Simultaneous measurements by ALIAS-II and other instruments on the same platform will allow an evaluation of the contribution of different catalytic cycles to ozone destruction. By measuring vertical profiles between 20 and 32 km, the data will help to determine the altitude at which heterogeneous chemistry ceases to affect the balance between the HO_x, ClO_x, and NO_x catalytic cycles. For added flexibility, ALIAS-II can be adapted to fly on a high-altitude remotely piloted aircraft (RPA) with only minor modifications.

2. INSTRUMENT DESCRIPTION

ALIAS-II is a two-channel, mid-infrared absorption spectrometer developed from the technology used on the ER-2 instrument ALIAS.[27] It is lighter (36 kg) and smaller ($6.6 \cdot 10^4$ cm^3, not including the absorption cell) than its four-channel predecessor because the absorption cell is open to the ambient airflow and because the forward optics are consolidated into a more compact space. The open cell removes the need for inlet probes or active flow control, eliminating the need for high-power pumps. Pumps create undesirable mechanical vibrations and require dissipating many kilowatts of heat through large radiator systems. Open-path spectroscopy eliminates problems due to wall chemistry that might perturb the measured concentrations of reactive species. The entire optical path from the ZnSe window in front of the lasers and detectors to the Herriott cell is enclosed in a purged optical chamber to prevent light absorption by air that is not in the open path between the two Herriott cell mirrors.

ALIAS-II uses second-harmonic absorption spectroscopy[28] to detect absorptions as small as 1 part in 10^5. As the source of mid-infrared radiation, each channel uses a tunable lead-salt diode laser (TDL) with a narrow laser linewidth to achieve a high spectral resolution of 0.0003 cm^{-1}. The TDLs are scanned across absorption lines at 10 Hz, with a superimposed modulation frequency (f) of 12 kHz on one channel and 14 kHz on the other. Direct absorption is measured by cold-shielded InSb photoconductive detectors mounted on an oxygen-free copper cold head along with the two TDLs inside a liquid nitrogen cooled dewar. The signal chains demodulate and filter the amplified signal from the detectors at $2f$ to yield second-harmonic spectra. 30 spectral scans are averaged to record one spectrum per channel every 3 seconds to a pressurized, ruggedized

hard disk along with engineering data. Every 60 seconds, pyrex cells with CaF_2 windows containing known concentrations of calibrated gas mixtures are mechanically moved into the optical path to record reference spectra. Carefully prepared standard gas mixtures provided by the National Oceanic and Atmospheric Administration (NOAA) Climate Monitoring and Diagnostics Laboratory (CMDL) are used in the reference cells to provide an accurate in-flight calibration standard. Power for the instrument when flying on the JPL OMS balloon gondola is supplied by lithium battery packs at 28 V DC producing 56 W on startup, < 50 W during normal operation. A separate array of batteries is used to power pulse-width-modulated resistive heaters that draw up to 250 W depending on the ambient temperature and insulation provided for the instrument. Figure 1 is a photograph of ALIAS-II in its original configuration designed for integration into RPAs. Development delays in the Perseus Aircraft required the package be retrofitted for a balloon platform for the flights in 1996-8.

A. Mechanical Design and Configuration

Original plans to deploy ALIAS-II on RPAs required that the two-channel spectrometer be extremely lightweight (36 kg) and use low power (50 W) because the ultimate altitude attainable by the RPA is severely limited by total payload mass. Figure 2 illustrates the open-path sample cell. The open cell considerably reduces mass and consists of a sturdy bulkhead that supports the near mirror and three invar rods that support the far mirror. Mass reductions in the balloon payload also greatly simplify launch activities through the use of a smaller balloon and increased launch opportunities

based on meteorological conditions. Due to the broad range of temperatures and pressures the package would encounter from sea level to over 32 km, thermal design with respect to optical and mechanical alignment is critical.

ALIAS-II is designed to preserve optical alignment through a broad range of atmospheric conditions and to withstand the shock of loading, launch, parachute shock and the rapid deceleration of landing which can be up to 10 G's in the balloon gondola. The configuration displayed in figure 1 is mounted on a 0.5-m x 0.57-m sheet of Hexcel 1.27-cm thick aluminum blue honeycomb tooling board, which has a density of 0.35 g/cc. This material was selected due to its extraordinarily high tensile strength to mass ratio and its certification for use in aircraft. Most of the other major components are made of 6061-T6 aluminum to ensure a similar coefficient of thermal expansion. Components are mounted to the Hexcel board using aircraft quality hardened inserts that are bonded into the board with high tensile strength structural epoxy. Retrofit of the aircraft package for use on the OMS *in situ* gondola required the package be separated into an electronics package and an optical package that could be deployed easily outside the gondola. The electronics package is mounted under the floor of the third level of the gondola and the optical package is mounted on a track and roller system on the top of the second floor of the gondola. The optical assembly is mounted on a 0.7-m x 0.6-m sheet of Hexcel tooling board. Lasers and detectors are mounted in a liquid nitrogen Dewar designed in collaboration with Kadel Engineering Corp. Careful design and meticulous construction allow this Dewar to have an extraordinarily long hold time of over 28 hours with only a 2.0-liter charge of liquid nitrogen. A rigid 6061-T6 aluminum mount secures the Dewar and optical chamber to the Hexcel base with eight 10-32 screws. A hermetically sealed optical chamber is bolted directly on the front of the Dewar and holds the steering mirrors

to inject and receive the laser beams into and out of the Herriott cell. 1.9 cm x 1.9 cm Newport Corp. ER2 coated mirrors are bonded to Newport MM-0.5 mounts on custom 6061-T6 aluminum posts inside the optical chamber. The reference cells and the Lucas Ledex H-1079-032 solenoid used to drive them are also mounted in the black anodized aluminum optical chamber. The reference cell carriage is mounted on a Precision Industries Corporation PB04-05 ball slide and is held in the retracted position by a stainless steel tension spring.

A precision machined bulkhead is fastened to the edge of the optical base plate to hold the Herriott cell near mirror and provide support for the three 0.95-cm diameter invar 66 rods which suspend the far mirror. A 0.17-cm diameter stainless steel support cable from the top floor of the gondola is used to provide additional support for the invar rods that suspend the far mirror. All aluminum components exposed to the sun during flight are painted using Deft 163-16 high reflective white catalyst paint to reduce solar heating. Prior to launching, the rolling optical bench is deployed to place the near mirror as close as possible to the edge of the gondola floor to ensure sampling clean air on ascent and descent. The bench is held in the deployed configuration with a 0.17-cm diameter steel cable wrapped twice around a 2.5-cm diameter capstan. One end of the cable is tied to the release latch and the other is run through a Lucas Ledex 195204-227 pull type solenoid. A Negator 2.3-kg constant force spring is used to retract the bench into the stowed position prior to the termination of a flight. The terminate sequence at the end of the flight calls for the solenoid to be activated just prior to the opening of the gondola parachute.

Active control of the resistive strip heaters at 25°C is initiated when the flight control program is running. Major components on the optical bench are insulated with

Nomex aramid fiber cloth and 5.1-cm-thick Styrofoam. Stable alignment of the laser beams is critical especially when passing through the tropopause region subjecting the payload to temperatures as low as -85°C in the tropics. The instrument electronics are less heavily insulated with only 2.5 cm-thick Styrofoam and Nomex covered with Kapton tape in order to prevent overheating on the ground and at float altitudes. Heat loss on ascent is primarily via efficient convection and conduction by air up to about 100 mbar. At higher altitudes radiative heat transfer becomes the dominant mode of transfer and a 35.6-cm x 30.5-cm radiation panel is used to dissipate the heat generated by the onboard 90 MHz Pentium processor, 16-bit A/D converter and drive transistors for the pulse-width-modulated resistive heaters. Heat from these high power components is conducted to the aluminum radiation panel with copper strips and special Gap Pad conductive heat sink compound. The radiation panel is recessed inside the gondola to shade it from the sun. Exposed parts of the instrument and critical optical supports are actively heated, but the key to conserving battery power is through adequate but not excessive insulation.

Figure 2 displays flight configuration with the Herriott cell deployed for launch. Prior to the deployment of the parachute the entire optical bench assembly is stowed inside the gondola. A stow command sent from the ground station fires the solenoid which releases a latch allowing the constant force spring to roll the bench along on delrin wheels which travel on 2.5-cm high aluminum rails. Once stowed, a spring-loaded latching mechanism designed to withstand a 10-G force ensures the instrument remains on the gondola after impact. Figure 3 shows the top view of the electronics box and the optical assembly, which are mounted separately inside the gondola.

B. Optical Design

There are four major subsystems of the ALIAS-II optical system: lasers and detectors are mounted in a liquid nitrogen cooled Dewar which is fitted with a X-Y-Z adjustable lens assembly, an optical chamber containing steering mirrors, a reference cell mechanism mounted on a precision linear ball slide, and an open-path Herriott cell. Within the open-path absorption cell, the infrared beams are reflected up to 86 times between two Au-Cr coated spherical zerodur mirrors.[29] This allows a relatively small cell (0.75 m or 1.5 m length) to contain an optical pathlength up to 120 meters, depending on the spacing of the mirrors. The long path length and 3- to 30-second scan averaging allow measurements of trace gases with detection sensitivities in the sub-ppbv range. Entrance and exit beams pass through the same hole in the near Herriott cell mirror, making the optical system very resistant to misalignment. Invar rods separate the spherical mirrors and the entire optical assembly is thermally stabilized to minimize the effects of thermal expansion. To minimize contamination of air passing through the optical path, the absorption cell is deployed outside the gondola prior to launch. Principal measurements are made during balloon decent (200 m/min.) sampling clean air flowing freely through the open cell. Figure 4 displays the mounting of the InSb detectors and lead-salt lasers on a single cold head in the Dewar and the optical chamber leading to the Herriott cell. Figure 5 displays the ray trace pattern of the beams on the Herriott cell mirrors.[30,31] The optical configuration of injecting the laser light into the same hole as the final ray exits provides an amazingly stable arrangement that makes the final design extremely resistant to misalignments. Commercial mirror mounts (Newport Corporation MM-0.5) are used to mount small steering mirrors to inject and receive the laser beams. Collimation and collection of the beams at the Dewar are achieved

using anti-reflection coated 1.27 cm ZnSe lenses mounted in adjustable black anodized aluminum barrel mounts.

C. Instrument Electronics

Digital electronics Data acquisition is controlled by an onboard computer featuring a highly integrated 80586 computer (Diversified Technology Model 3010) running at 90 MHz and a bootable 540 Mb ruggedized hard disk. The 3010 computer is mounted in a passive backplane along with a custom 16-bit signal averager, a National Instruments 16-bit A/D converter model ATMIO16XE, a custom Digital I/O board, a custom analog monitor board, a 3COM 509 ethernet card, and a Mach 32 video card. A separate analog electronics box next to the main computer contains the custom current supply board which controls the current scans for the lasers and a custom signal chain with adjustable gain stages and bandpass filters for the signals from the laser detectors. Figure 6 displays the various electronic components of ALIAS-II. While on the ground for calibration and pre-flight checkout a keyboard and monitor are connected to the instrument to display the spectra from both channels and vital engineering data.

The custom digital I/O board provides the timing for the main data acquisition program and controls the commands to the various instrument components through four Intel 82C55 programmable interfaces. The custom-designed analog monitor works in conjunction with the National Instruments ATMIO16XE 16-bit A/D converter to provide the sensor biasing, conditioning, and signal input. Sensors are provided to monitor the following: two silicon diodes on the laser cold head to monitor its temperature; two

thermistors to monitor the sample air temperature; a 0-1000 Torr absolute baratron to monitor the sample pressure; 12 nickel-iron resistive temperature devices (RTDs) at strategic monitor points on the instrument; and 12 heater voltages to monitor the load on the various heater circuits.

Signals from the custom-designed signal chains are passed on to the custom-designed 16-bit signal averager which is also mounted in the passive backplane of the computer box. This board acquires 2 channels of dc and two channels of ac analog data from the signal chain, consisting of 1024-point spectra from each channel. The heart of the 16-bit signal averager are the Crystal Semiconductor 5336 analog to digital stereo converters that acquire the dc and ac analog signals simultaneously. The digitized signals are then sent to memory modules on the same board to allow the main CPU to monitor other functions while spectra are being acquired.

Analog Electronics The analog electronics are packaged in two separate boxes shielded from the noisy high speed digital components. The first box contains custom-designed transgalvanic preamplifiers for the Indium Antimonide (InSb) detectors and is mounted directly on the Dewar to minimize the distance between the detectors and the preamplifiers. The second analog box contains the custom-designed current supplies and signal chains with digital counters to generate the TDL modulation-demodulation frequencies as shown in figure 6.

During flight the data collection is controlled by scanning each TDL through an isolated absorption line of each species of interest at 10 Hz. Each TDL is turned off for a period of 1 ms at the beginning of each 0.1 s ramp to provide an accurate 800 μs auto-zero trace for the null circuit as well as providing an accurate zero absorption reference.

100 μs after the beginning of this brief TDL-off period a trigger is sent to the custom 16-bit signal averager to begin data acquisition. This method of nulling allows the circuit to accommodate both changes in background light levels and detector impedance through the flight.

Each TDL current supply has a four-output, 16-bit digital-to-analog converter. Two of the outputs are used to generate starting current up to 2.0 Amps. One output is used to charge a capacitor with a constant current, generating a voltage that is linear with time. The ramp is reset once each 0.1 s to give a 10 Hz spectral scan rate. The last output is chopped at the TDL current-modulation frequency to make a square wave with controllable amplitude. The resulting square wave is filtered through a bandpass filter to keep only the sinusoidal fundamental. The starting voltage, ramp voltage, and modulation are summed together in a current feedback loop to generate the current on the TDL. Modulation frequencies of 12 and 14 kHz are used, with phase shifts introduced to phase in accurately the demodulators which are set for $2f$ detection at 24 and 28 kHz.

The signal chains receive the dc-coupled preamp outputs and split them into dc and ac components for each TDL-detector pair. The dc signal chain has programmable gains of 1, 2, 4,...128 and a high-Q, low-pass filter with a bandpass of approximately 5 kHz. The ac signal chain has a small amount of fixed gain, programmable gains of 1, 2, 4,...2048, and a high-Q bandpass filter centered around the respective $2f$ demodulation frequencies. After the signal gain stages there is a demodulation stage operating at the $2f$ detection frequency and then a post demodulator high-Q, low-pass filter with a bandpass of 5 kHz.

Thermal control of critical components is necessary to maintain optical alignment of the instrument and stability of the instrument electronics. A pulsed width modulated

temperature control circuit is used to keep these critical components at 25°C during the duration of the flight. All heater control circuits are proportional controllers that use nickel-iron resistance temperature detectors (Minco S39FAY36B, 604 Ohm ±0.26% at 0°C).

Gondola Interface The interface to the gondola electronics was designed and fabricated to isolate the instrument as much as possible from the gondola Control Interface Package (CIP). Commands sent to the gondola and instruments on board are sent through the CIP and it is critical to avoid interference with the control systems. Down link telemetry of data is also transferred through the CIP at 9600 baud via an RS232 connection. Power for the instrument and heaters is switched on and off by commands relayed through the CIP. A separate command is used to fire the retraction relay for the optical bench before termination of the flight. The 28-V supplied by the battery packs is conditioned using Vicor DC-DC power converters and ripple attenuator modules (RAMs) to minimize interference from the gondola electronics. As shown in figure 6 ALIAS-II sends data through an RS232 connection to the constant bandwidth voltage controlled oscillator (VCO) in the gondola CIP. The VCO transmits the data by radio at 1.5 GHz to a receiving station on the ground. There, signals of the six different instruments onboard the gondola are separated from each other by an electronic discriminator and converted to a bipolar voltage signal sent over a RS232 connection to a custom-built input module. The input module uses a Maxim RS232 converter allowing the data to be directly read into the COM2 port on the Dell 200 MHz ground support station. A second converter is used to simultaneously record data on the VS4000 providing two copies of the data during flight.

D. INSTRUMENT SOFTWARE

ALIAS-II uses an on-board bootable 540-Mb hard disk and is controlled by a single executable program that runs using the MSDOS 6.0 operating system. The control program governs the scanning of the lasers, data acquisition, and the various engineering requirements. It may be initiated in two independent modes: one for setup and calibration on the ground, and the other for data collection during flight. The software is written in the C++ programming language and uses a library of low-level graphics routines to display the AC and DC scans of each laser as well as engineering temperature and pressure data. Commands are entered at the keyboard to select the optimum parameters of laser scan range, laser heater voltage, modulation intensity, and gain settings for both channels before flight and these parameters are stored in a parameter file.

The fixed timing sequence for the data acquisition cycle is illustrated in figure 7. The lasers are scanned at 10 Hz and each TDL is turned off for 800 μs at the beginning of each scan to ensure an accurate background signal. After a suitable delay following this brief TDL-off period (to allow stabilization of the TDL output) a trigger pulse is generated by the hardware to initiate the collection of spectra by the custom-designed 16-bit signal averager (SA) board. The programable CPU on the 16-bit SA operates independent of the main 80586 CPU which runs the ALIAS-II control software. The 16-bit SA board collects data as prescribed by a resident program that is downloaded during program initialization. Thirty individual 0.1-s spectra are acquired from the AC and DC channel for each laser to produce four 1024-point spectra. The averaged spectra are transferred to the main control program, as they become available, every 3 seconds. Because the signal averager operates independently of the main 80586 CPU, the software

control of engineering parameters is carried on simultaneously with the acquisition of data during the 3 seconds that are available while the spectra are being averaged. In this way the atmospheric spectral data and instrument control functions run simultaneously.

Data are written continuously to the on-board hard disk and simultaneously sent out via the RS-232 port to be downlinked to the receiving station on the ground. The files on the hard disk are segregated into files according to the file structure illustrated in figure 7. Each file contains approximately 5 min of flight data and represents ten full frames of data. Each 30-s frame consists of ten subframes, and each subframe consists of individual 3-s averaged spectra for each of the 4 ALIAS-II channels. Appended to each subframe is a 1-kbyte housekeeping data block containing up to 512 values for engineering data and science data words. At 60-s intervals the reference cells are moved into the beam to record an in-flight standard reference signal. A second check is made 30 seconds later of the direct absorption signal by turning the laser modulation off and provides a second in flight calibration of the $2f$-absorption signal. These reference scans form the tenth subframe of each frame. The reference spectra are used in post-flight data processing to compensate for any drifts in the laser or electronics temperature during flight and for wavelength calibration and line identification. A typical 6-hour flight generates approximately 60 megabytes of raw data, representing more than 19,000 individual spectra.

Parameter files containing hardware settings and laser scan parameters are contained in the same directory as the main ALIAS-II control program. The parameter file is read in by the control program during the initialization and written to a structure (or table) within the program. This parameter file contains values for the TDL scan currents, modulation amplitudes, signal chain gains, and the file structure parameter (number of

frames, subframes, atmospheric subframes, and reference subframes that define one file). At initialization the hardware is configured according to the values in the parameter table. In the ground mode the software flags any user-entered commands that are changed and the parameter table may be rewritten at any time. This sets the hardware parameters that will be initialized at the next power up of the instrument. This allows final tuning of the laser scans and signal chain gains during the preflight checkout on the flight line before launch, and a new parameter file can be saved for in-flight initialization.

E. Calibration and Data Processing

Calibration and postflight data processing procedures were developed at the Jet Propulsion Laboratory and are detailed in separate publications.[27,28] After the termination of a flight the hard disk is easily removed from the instrument and the data is transferred to a Digital VAX Station 4000 for rapid reduction to obtain volume mixing ratios. Briefly, Beer's law is used to extract a volume density based on the observed absorption. However, the relatively low concentration of various chemicals in the stratosphere produces very weak line center absorptions. Applying high frequency modulation ($f = 12$ or 14 kHz) to the laser current supply ramp and detecting the absorption at $2f$ improves signal-to-noise ratios producing second harmonic line shapes.[32] Great care is taken to ensure that the instrument electronics produce a linear response to the return laser power on the detectors. Careful calibration yields a response number, R, for each signal channel and is defined as:[27]

$$R_i = \left[\frac{H_2(\text{obs})A(\text{calc})}{H_2(\text{calc})A(\text{obs})}\right]\left(\frac{DC_g}{AC_g}\right)\left(\frac{1}{P'}\right),$$

where A is the direct absorption signal level and H_2 is the $2f$ signal level. $P' = (P-P_0)$ is the total power level above the zero level P_0 and AC_g and DC_g are the AC ($2f$) and DC (direct) amplifier gain values.

Normalized $2f$ spectra are converted to useable spectroscopic units once R_i has been determined as follows:

$$H_j(v) = y_j\left(\frac{1}{R_i P_j'}\right)\left(\frac{DC_g}{AC_g}\right),$$

where y_i (j = 1,1024) is the observed $2f$ spectrum and R_i is the response number for channel i. The factor $1/P'$ normalizes the signal to the returned TDL power. A mixing ratio can be derived by fitting a synthetic spectrum to the observed spectrum with the best line parameters and modulation amplitudes once converted to spectroscopic units (H_2 versus inverse centimeters). For preliminary post-flight data analysis, least-squares fitting of each spectrum is not tractable due to the large number (nearly 19,000 individual spectra may be recorded during a flight) of spectra. To reduce processing time a matrix containing calculated peak-to-peak $2f$ signal sizes is generated for each absorption line to be measured for a fixed mixing ratio close to that expected during flight for a broad temperature and pressure range covering the expected fight track. The grid size for these calculations is typically 1 K in temperature and 1 mbar in pressure. After converting each spectrum to spectroscopic units the appropriate matrix is consulted to obtain the synthetic

peak-to-peak $2f$ signal amplitude with the measured Herriott cell temperature and pressure. The observed mixing ratio, σ(obs), is then obtained by comparing σ(obs) to σ(calc) times the ratio of the observed $2f$ signal size, H_2 (obs), to the calculated $2f$ signal size H_2 (calc).

$$\sigma(\text{obs}) = \frac{H_2(\text{obs})}{H_2(\text{calc})}\sigma(\text{calc})$$

The calibrations are verified many times over the entire pressure range of the flights (500 to 5 mb) using standards provided by J. W. Elkins of the National Oceanic and Atmospheric Administration (NOAA) Climate Monitoring and Diagnostics Laboratory (CMDL) in the following concentrations:

Cylinder CA-2789

276.5 ±3 ppbv N_2O

1150.9 ±12 ppbv CH_4

193.9 ±4 ppbv CO

balance: zero air

The results of these pump down calibrations confirm that the instrument accuracy is ±3% and precision is on the order of 1%. Of course the flight environment is considerably harsher than the calibration conditions and the accuracy and precision suffer due to decreased laser return power during flight and interference from other instruments

and the gondola electronics. Conservative estimates of the instrument precision and accuracy in its first series of flights are listed in Table 1.

Figure 8 includes representative spectra from the flight of February 14, 1997, over Juazeiro do Norte, Brazil at 62.2 mbar for N_2O at 2207.6204 cm^{-1} recorded using channel 1 and quartet of CH_4 at 2947.66785, 2947.81081, 2947.91211, and 2948.10781 cm^{-1} on channel 2. Laser return powers, peak-to-peak signal intensities, ambient temperature, pressure, and GMT are also downlinked via telemetry to the NSBF base to record data in real time during flight in case the payload is damaged or lost. Primary data reduction is completed after the ruggedized hard disk is recovered. The data recovered on board are traditionally cleaner than the data transmitted via telemetry due to EMI with the telemetry data. The flight data are rapidly processed using the VS4000 and compared to synthetic spectra generated using the 1996 AFGL line list to produce vertical profiles of N_2O and CH_4 (figure 9). In all flights the CH_4 ascent volume mixing ratio was noticeably less than the descent data and this result is still under investigation. The descent data are assumed to be the better value as the gondola and instrument are passing through clean air. The discrepancy with the ascent data probably reflects a dilution of the chemical species as the balloon and payload passes through the air parcel or is an instrumental artifact. It should also be noted that the temperatures encountered by the payload at the tropopause are quite cold (-70 to -86°C) and are in the regime of large uncertainty in the temperature broadening coefficients of the AFGL line lists. This introduces higher uncertainty in the CH_4 volume mixing ratio presented in figure 9 and further laboratory work is in progress to improve the low temperature data. Flight dates and locations for the OMS and POLARIS campaigns are listed in Table 2.

Compact correlation plots of CH_4 *vs.* N_2O demonstrate that they are in "slope equilibrium," which means that their correlation is independent of location along the surface of fastest mixing.[33] Figure 10 displays the mid-latitude CH_4 *vs.* N_2O correlation for ALIAS-II, Mark IV, and ALIAS-I on the ER-2. ALIAS-II was launched from Ft. Sumner at sunrise on September 21, 1996 and ALIAS-I flew close to Ft. Sumner later that same day. The Mark IV flew from Ft. Sumner on September 28, 1996. Figure 11 is a CH_4 *vs.* N_2O correlation plot for the flights completed in the OMS/STRAT/POLARIS campaigns in 1996/97. Note that these values agree well with ATMOS data.[34]

Tracer gases with long photochemical lifetimes like CH_4 and N_2O will often have linear relationships if the photochemical lifetimes are longer than the vertical transport times.[34] If the mixing is slow between different latitudes with different photochemical environments the correlations between these tracers with be quite different at different latitudes as shown in figures 9 and 11. These differences in the tracer vs. tracer correlations have been observed in the tropics and extra-tropics.[35,36] This led to the development of the "tropical pipe" model of circulation in the stratosphere where the tropical stratosphere is isolated from the extra-tropics.[37] Lower than expected tracer concentrations in the tropical stratosphere show that there is indeed transport of tracers originating in mid-latitudes through the sub tropical barrier.[38] Using the results from the tropical and extratropical OMS flights we were able to calculate the fraction of extra-tropical air entrained into the tropical stratosphere is 50% (+18%, -30%) at 20 km (θ = 500 K), increasing to 78% (+11%, -19%) at 28 km (θ = 770 K).[6] This is a similar result to those of other studies.[36,4] These results have important implications for calculated trends of mid-latitude ozone and the dilution of NO_y emissions in the atmosphere from civil aviation. Once transported into the tropical stratosphere the NO_y is efficiently lofted

to higher altitudes where its potential for ozone destruction is much greater. Using the CH_4 *vs.* N_2O correlations it is possible to provide constraints for multi-dimensional models used to calculate the impacts of anthropogenic gases in the atmosphere.

Further work is in progress to improve the agreement between the various platforms through careful low temperature laboratory studies of the specific spectral parameters. Second generation electronics are also being implemented to improve precision and reliability. Design of an improved optical chamber is also in progress, which will stabilize the return laser power over the large temperature and pressure range of the balloon flights. The photochemically important species HCl and NO_2 may also be measured with ALIAS-II to compliment the instruments used in the upcoming SAGE III Ozone Loss and Validation Experiment (SOLVE). The open-path design will allow *in situ* measurements that will not be influenced by surface or wall effects. These measurements will help validate the measurements of the SAGE III satellite which is the latest in a family of solar occultation satellite instruments designed to monitor distributions of stratospheric and upper tropospheric aerosol, ozone, water vapor, and nitrogen dioxide (see http://arbs8.larc.nasa.gov/). The ALIAS-II instrument and JPL's Atmospheric Laser Spectroscopy Group may be viewed at http://laserweb.jpl.nasa.gov/.

ACKNOWLEDGMENTS

The authors wish to thank NASA's Upper Atmospheric Research Program (UARP) Code Y manager Dr. Michael J. Kurylo and the High-Speed Research Program (HSRP) for supporting this project. Significant contributions to the ALIAS-II instrument design, fabrication, and field operations were also made by W. Steve Woodward, Matthew A. Tuchscherer, Linley A. Kroll, Katayoon Modarress, Robert McMillan, Miroslav Vondrus, James Swanson, and the JPL Space Instruments Machine Shop. James J. Riccio, Ronald D. Howe, Jose J. Landeros, and W. Blake Wilson of the Jet Propulsion Laboratory's balloon support facility working with the expert staff at NSBF provided us with seven picture perfect launches. Photograph in figure 1 provided by Tom Wynne at JPL. G. C. Toon provided the Mark IV data in figure 10. Special thanks are given to William Brune for his work as Project Scientist for the Observations from the Middle Stratosphere (OMS) campaigns, and to James W. Elkins and Richard Meyers for providing CO, N_2O, and CH_4 gas standards. The research described in this publication was carried out by the Jet Propulsion Laboratory, California Institute of Technology, under contract with the National Aeronautics and Space Administration.

[1] P. D. Goldan, W. C. Kuster, A. L. Schmeltekopf, F. C. Fehsenfeld, and D. L. Albritton, "Correction of Atmospheric N_2O Mixing-Ratio Data," J. Geophys. Res. **86**, 5385-6, (1981).

[2] Y. A. Bush, A. L. Schmeltekopf, F. C. Fehsenfeld, and D. L. Albritton, "Stratospheric Measurements of Methane at Several Latitudes," Geophys. Res. Let. **5**, 1027-9, (1978).

[3] A. E. Roche, J. B. Kumer, J. L. Mergenthaler, G. A. Ely, W. G. Uplinger, J. F. Potter, T. C. James, and L. W. Sterritt, "The Cryogenic Limb Array Spectrometer (CLAES) on UARS: experiment description and performance," J. Geophys. Res. **98**, 10,763-76, (1993).

[4] K. Minschwaner, A. E. Dessler, J. W. Elkins, C. M. Volk, D. W. Fahey, M. Loewenstein, J. R. Podolske, A. E. Roche, and K. R. Chan, "Bulk properties of isentropic mixing into the tropics in the lower stratosphere," J. Geophys. Res. **101**, 9433-9, (1996).

[5] M. R. Gunson, M. M. Abbas, M. C. Abrams, M. Allen, L. R. Brown, T. L. Brown, A. Y. Chang, A. Goldman, F. W. Irion, L. L. Lowes, E. Mahieu, G. L. Manney, H. A. Michelsen, M. J. Newchurch, C. P. Rinsland, R. J. Salawitch, G. P. Stiller, G. C. Toon, Y. L. Yung, and R. Zander, "The Atmospheric Trace Molecule Spectroscopy (ATMOS) experiment: Deployment on the ATLAS Space Shuttle missions," Geophys. Res. Let. **23**, 2333-6, (1996).

[6] R. L. Herman, D. C. Scott, C. R. Webster, R. D. May, E. J. Moyer, R. J. Salawitch, Y. L. Yung, G. C. Toon, B. Sen, J. J. Margitan, K. H. Rosenlof, H. A. Michelsen, J. W. Elkins, "Tropical entrainment timescales inferred from stratospheric N_2O and CH_4 observations," Geophys. Res. Lett. **25**, 2781-4 (1998).

[7] Stolarski, R. S., and H. L. Wesoky, "The Atmospheric Effects of Stratospheric Aircraft: A Fourth Program Report," NASA Reference Publication 1359, (1995).

[8] WMO, 1991; ICAO, 1991; S. W. Kandebo, "HSCT engine research makes steady gains," Aviation Week & Space Tech. Sept. 13, 46-50 (1993); J. P. Beck, C. E. Reeves, F. A. A. M. De Leeuw, and S. A. Penkett, "The effect of aircraft emissions on tropospheric ozone in the Northern Hemisphere," Atmos. Environ. **26A**, 17-29 (1992); D. F. Ehhalt, F. Rohrer , and A. Wahner, "Sources and distribution of NO_x in the upper troposphere at northern mid-latitudes," J. Geophys. Res. **97**, 3725-38 (1992); U. Schumann, Editor, "Air traffic and the environment- Background, tendencies and potential atmospheric effects," in Proceedings of a DLR international colloquium, Bonn, Germany, November 15-16, Springer-Verlag, Berlin (1990).

[9] P. J. Crutzen, "The influence of nitrogen oxides on the atmospheric ozone content," Quart. J. Roy. Met. Soc. **96**, 320, (1970).

[10] H. S. Johnston, "Reduction of stratospheric ozone by nitrogen oxide catalysts from SST exhaust," Science **173**, 517, (1971).

[11] P. J. Crutzen, "The role of NO and NO_2 in the chemistry of the troposphere and stratosphere," Ann. Rev. Earth & Planet. Sci. **7**, 443, (1979).

[12] C. Johnson, J. Henshaw and G. McInnes, "Impact of aircraft and surface emissions of nitrogen oxides on tropospheric ozone and global warming," Nature **355**, 69-71, (1992); Th. Peter, C. Brühl, and P. J. Crutzen, "Increase in the PSC-formation probability caused by high-flying aircraft," Geophys. Res. Lett. **18**, 1465-68 (1991); S. Bekki and J. A. Pyle,"Potential impact of combined NOx and SOx emissions from future high speed civil transport aircraft on stratospheric aerosols and ozone," Geophys. Res. Lett. **20**, 723-6 (1993); P. Kasibhatla, "NOy from sub-sonic aircraft emissions: A global three-dimensional model study," Geophys. Res. Lett. **20**, 1707-10 (1993).

[13] D. W. Fahey, E. R. Keim, E. L. Woodbridge, R. S. Gao, K. A. Boering, B. C. Daube, S. C. Wofsy, R. P. Lohmann, E. J. Hintsa, A. E. Dessler, C. R. Webster, R. D. May, C. A. Brock, J. C. Wilson, R. C. Miake-Lye, R. C. Brown, J. M. Rodriguez, M. Loewenstein, M. H. Proffitt, R. M. Stimpfle, S. Bowen, and K. R. Chan, "In situ observations in aircraft exhaust plumes in the lower stratosphere at mid-latitudes," J. Geophys. Res. **100**, 3065-74 (1995).

[14] K. A. Boering, B. C. Daube, Jr., S. C. Wofsy, M. Loewenstein, J. R. Podolske, and E. R. Keim, "Tracer-tracer relationships and lower stratospheric dynamics: CO_2 and N_2O correlations during SPADE, Geophys. Res. Lett. **21**, 2567-70, (1994).

[15] F. L. Moore, J. W. Elkins, E. A. Ray, G. S. Dutton, R. Dunn, D. W. Fahey, R. McLoghlin, T. L. Thompson, "First in situ gas chromatograph on a balloon platform yielding tracer measurements with improved spatial resolution," in preparation for J. Geophys. Res. (1998).

[16] M. H. Proffitt and R. J. McLaughlin, "Fast-response dual-beam UV-absorption ozone photometer suitable for use on stratospheric balloons," Rev. Sci. Instrum. **54**, 1719-28, (1983).

[17] S. J. Oltmans and D. J. Hofmann, "Increase in lower-stratospheric water-vapor at a mid-latitude northern-hemisphere site from 1981 to 1994," Nature **374**, 146-49, (1995).

[18] H. Jost, M. Loewenstein, L. Pfister, J. J. Margitan, A. Y. Chang, R. J. Salawitch, H. A. Michelsen, "Laminae in the tropical middle stratosphere: Origin and age estimation," Geophys. Res. Lett. 25, 4337 (1998).

[19] K. A. Boering, A. E. Andrews, B. C. Daube, S. C. Wofsy, M. Loewenstein, C. R. Webster, and J. W. Elkins, "Time scales for stratospheric transport inferred from in situ measurements of CO_2 from aircraft and balloons," in preparation for J. Geophys. Res. (1998).

[20] C. A. Reber, "The Upper Atmosphere Research Satellite," Geophys. Res. Lett. **20**, 1215-18 (1993).

[21] C. B. Farmer, "High resolution spectroscopy of the sun and the Earth's atmosphere from space," Michrochim. Acta [Wien] III, 189-214 (1987).

[22] C. B. Farmer and O. F. Raper, "Final report on the first flight of the ATMOS instrument during the spacelab 3 mission, April 29 through May 6, 1985," JPL Publication **87-32**, 1-45 (1987).

[23] R. Stachnik, "Submilimeterwave emission measurements of ozone, HCl, H_2O, and HNO_3 during POLARIS," in preparation for Geophys. Res. Lett. (1998).

[24] G. C. Toon, "The JPL MkIV interferometer," Optics & Photonics News **2**, 19-21, (1991).

[25] C. R. Webster, R. D. May, D. W. Toohey, L. M. Avallone, J. G. Anderson, P. Newman, L. Lait, M. R. Schoeberl, J. W. Elkins, and K. R. Chan, "Chlorine chemistry on polar stratospheric cloud particles in the arctic winter," Science **261**, 1130-34 (1993).

[26] C. R. Webster and R. D. May, "Simultaneous *in situ* measurements and diurnal variations of NO, NO_2, O_3, jNO_2, CH_4, H_2O, and CO_2 in the 40- to 26-km region using an open path tunable diode laser spectrometer," J. Geophys. Res. **92**, 11931-50 (1987).

[27] C. R. Webster, R. D. May, C.A. Trimble, R. G. Chave, and J. Kendall, "Aircraft (ER-2) laser infrared absorption spectrometer (ALIAS) for in situ stratospheric measurements of HCl, N_2O, CH_4, NO_2 and HNO_3," Appl. Opt. **33**, 454-72 (1994).

[28] R. D. May and C. R. Webster, "Data processing and calibration for tunable diode laser harmonic absorption spectrometers," J. Quant. Spectrosc. Radiat. Transfer **49**, 335-47 (1993).

[29] J. Altman, R. Baumgart, and C. Weitkamp, "Two-mirror multipass absorption cell," Appl. Opt. **20**, 995-99 (1981).

[30] D. Herriott, H. Kogelnik, and R. Kompfner, "Off-Axis Paths in Spherical Mirror Interferometers," Appl.Optics **3**, 523-6 (1964).

[31] R. L. Herman, "*In Situ* Measurements of Chemical Tracers in the Stratosphere; CO, N_2O, and CH_4," Ph.D Thesis, California Institute of Technology (1998).

[32] C. R. Webster, R. T. Menzies, and E. D. Hinkley, "Infrared laser absorption: theory and applications in Laser Remote Chemical Analysis," R. M. Measures, ed. (Wiley, New York, 1988); 163-272.

[33] R. A. Plumb and M. K. W. Ko, "Interrelationships between mixing ratios of long-lived stratospheric constituents," J. Geophys. Res. **97**, 10145-56, (1992).

[34] H. A. Michelsen, G. L. Manney, M. R. Gunson, C. P. Rinsland, and R. Zander, "Correlations of stratospheric abundences of CH_4 and N_2O derived from ATMOS measurements," Geophys. Res. Lett. **25**, 2777-80 (1998).

[35] D. M. Murphy, D. W. Fahey, M. H. Proffitt, S. C. Liu, K. R. Chan, C. S. Eubank, S. R. Kawa, and K. K. Kelly, "Reactive nitrogen and its correlation with ozone in the lower stratosphere and upper troposphere," J. Geophys. Res. **98**, 8751-73, (1993).

[36] C. M. Volk, J. W. Elkins, D. W. Fahey, R. J. Salawitch, G. S. Dutton, J. M. Gilligan, M. H. Proffitt, M. Loewenstein, J. R. Podolske, K. Minschwaner, J. J. Margitan, and K. R. Chan, "Quantifying transport between the tropical and mid-latitude lower stratosphere," Science **272** 1763-8, (1996).

[37] R. A. Plumb, "A "tropical pipe" model of stratospheric transport," J. Geophys. Res. **101**, 3957-72, (1996).

[38] L. M. Avallone and M. J. Prather, "Photochemical evolution of ozone in the lower tropical stratosphere," J. Geophys. Res. **101**, 1457-61, (1996).

Table 1. Estimated precision and accuracy

ALIAS-II (Balloon) (any 2 Channels)	species measured		Precision	accuracy*	Time
	Nitrous oxide	N_2O	1.0 ppbv (± 1%)	10 ppbv (± 5%)	3 sec
	Methane	CH_4	10 ppbv (± 1%)	50 ppbv (± 5%)	3 sec
	Carbon monoxide	CO	0.2 ppbv (± 2%)	0.5 ppbv (± 5%)	3 sec
	Hydrochloric acid	HCl	0.1 ppbv (± 5%)	0.15 ppbv (± 10%)	30 sec
	Nitrogen dioxide	NO_2	0.05 ppbv (± 5%)	0.10 ppbv (± 10%)	30 sec

*weighted for expected signal-to-noise for 100 ppbv N_2O, 1.0 ppm CH_4, 10 ppbv CO, 2.0 ppbv HCl, and 1.0 ppbv NO_2 at 25 km.

Table 2. Flights of the OMS Balloon Payload.

Flight date (yymmdd)	Location	Latitude	Longitude
960610	Ft. Sumner, NM	34° N	104° W
960921	Ft. Sumner, NM	34° N	104° W
970214	Juazeiro do Norte, Ceará, Brazil	7° S	39° W
970630	Fairbanks, AK	65° N	148° W
971111	Juazeiro do Norte, Ceará, Brazil	7° S	39° W
971120	Juazeiro do Norte, Ceará, Brazil	7° S	39° W
980518	Ft. Sumner, NM	34° N	104° W

Figure Captions

1. ALIAS-II configured for an aircraft platform.

2. Top view of ALIAS-II in the balloon gondola, with the optical assembly shown in both deployed and stowed positions. The hatched area is the ALIAS-II electronics, which are mounted above the optical assembly.

3. Diagram of ALIAS-II (top view). The optical assembly and electronics box are mounted separately inside the balloon gondola.

4. Optical ray trace through ALIAS-II. Infrared laser beams are shown as dashed lines. Optical components such as windows, lenses, and mirrors are outlined with thick lines.

5a. Near mirror: spot patterns created at the intersection of the infrared beams and the reflective surface of the near mirror of the Herriott cell. The infrared beams enter and exit the Herriott cell through a tapered hole at spot number 86 (shaded). Note: top of mirror is at the left.

5b. Far mirror spot patterns. With 86 passes, C_{43v} is the symmetry point group of the beams in the Herriott cell. However, the angle between consecutive spots on the same mirror is almost 120°, so the point group is almost C_{3v}.

6. ALIAS-II electronics. CIP, Control Interface Package; NSBF, National Scientific Balloon Facility; GPS, Global Positioning System; IMOD, laser current modulation amplitude; RTDs, resistive temperature devices.

7. Timing diagram for laser current ramp, null integrator, and ramp reset. File structure for the data acquisition software is also displayed showing the file structure, frame, and subframe content.

8. One frame of atmospheric N_2O and CH_4 spectra recorded at 62 mbar over Brazil on February 14, 1997. Lasers are scanned over absorption lines at 10 Hz and 30 individual spectra are averaged into a subframe, which is written to disk every 3 seconds (cf. Fig. 7).

9. Volume mixing ratio profiles of CH_4 and N_2O retrieved by ALIAS-II on February 14, 1997, over Juazeiro do Norte, Brazil and on June 30, 1997, over Fairbanks, Alaska. Extremely high values of both tracers CH_4 and N_2O were recorded at float altitudes near 32 km in the tropics indicating vertical transport into the middle stratosphere. The polar vortex filaments, which were also sampled by ER-2 instruments, indicate downward transport of older air in the polar vortex.

10. CH_4 *vs.* N_2O correlation for ALIAS-II on the OMS gondola flown out of Ft. Sumner, New Mexico and ALIAS-I on the ER-2 flown out of NASA Ames Research Center, California on September 21, 1996. The MarkIV was flown out of Ft. Sumner on September 28, 1996.

11. CH_4 *vs.* N_2O from ALIAS-II and fits to ATMOS data sets.[34]

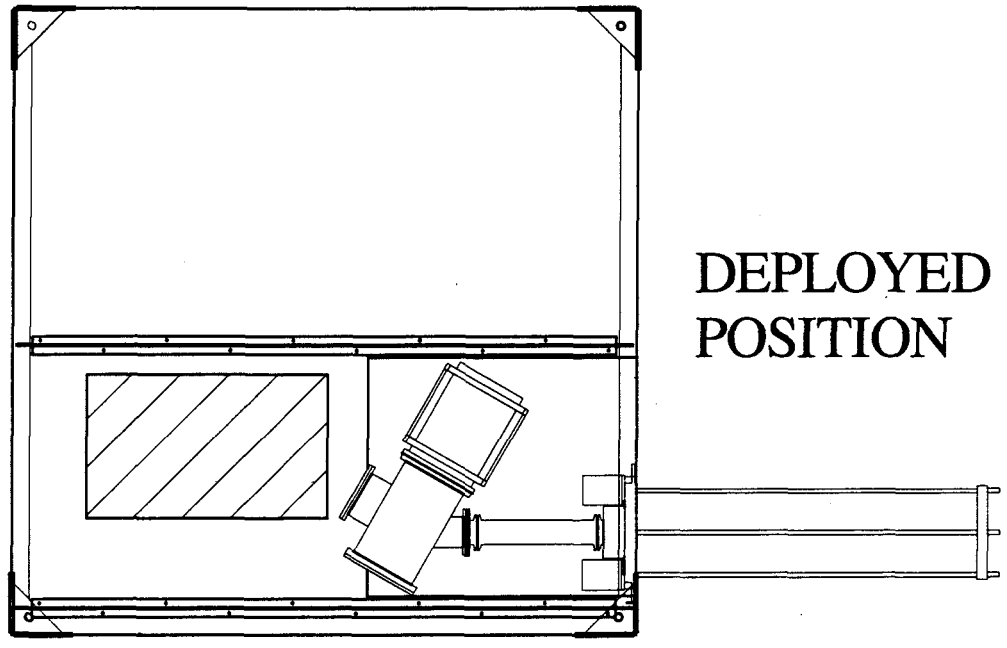
DEPLOYED
POSITION

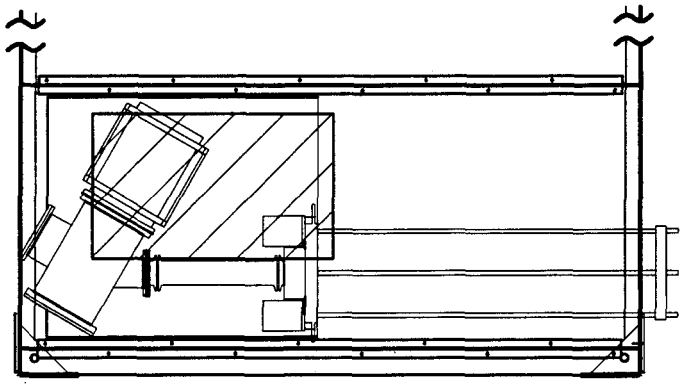
STOWED
POSITION

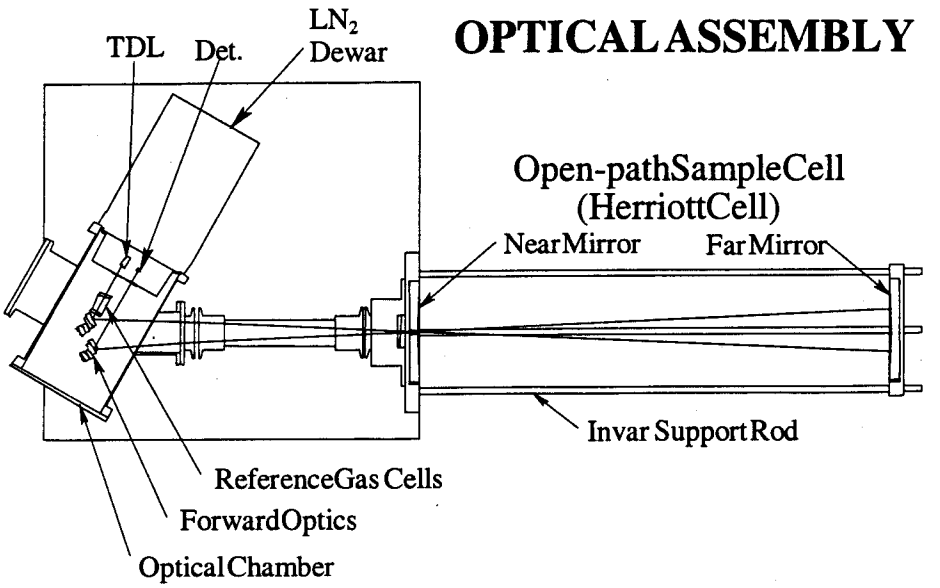
OPTICAL ASSEMBLY
TDL
Det.
LN_2 Dewar
Open-path Sample Cell
(Herriott Cell)
Near Mirror
Far Mirror
Invar Support Rod
Reference Gas Cells
Forward Optics
Optical Chamber

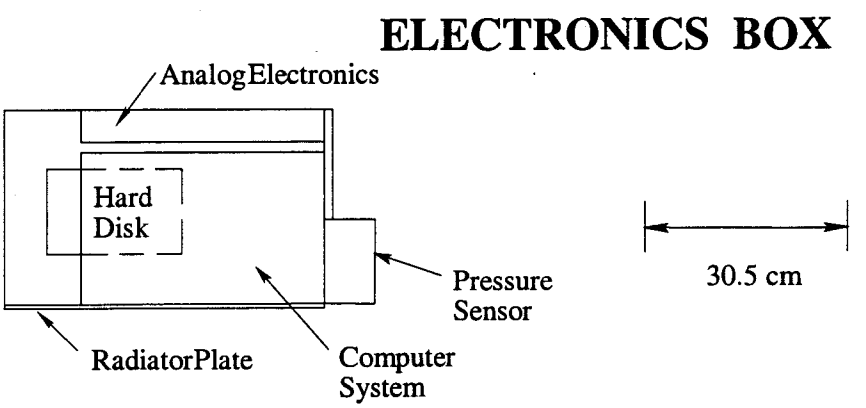
ELECTRONICS BOX
Analog Electronics
Hard Disk
Pressure Sensor
30.5 cm
Radiator Plate
Computer System

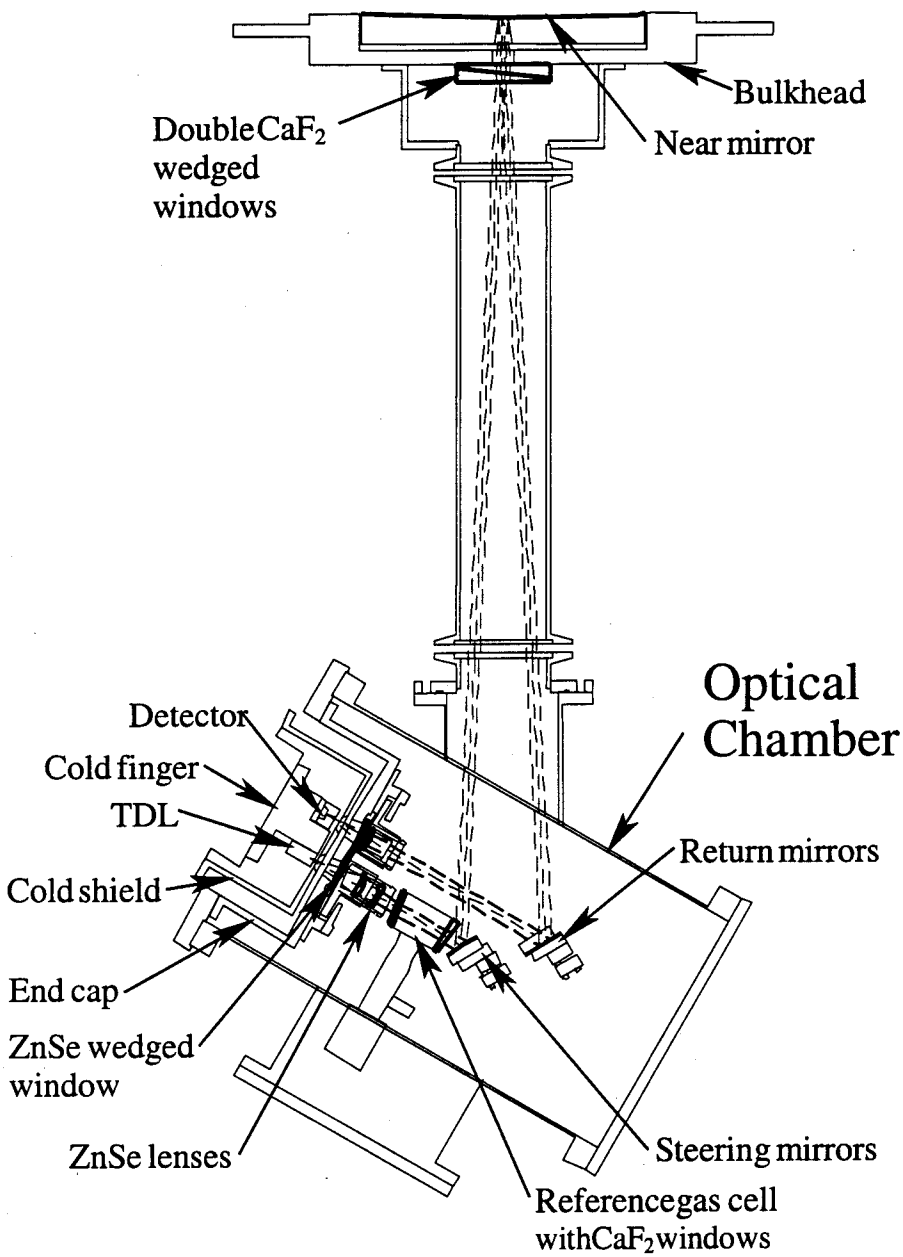
Bulkhead
Double CaF_2 wedged windows
Near mirror
Optical Chamber
Detector
Cold finger
TDL
Cold shield
Return mirrors
End cap
ZnSe wedged window
ZnSe lenses
Steering mirrors
Referencegas cell withCaF_2windows

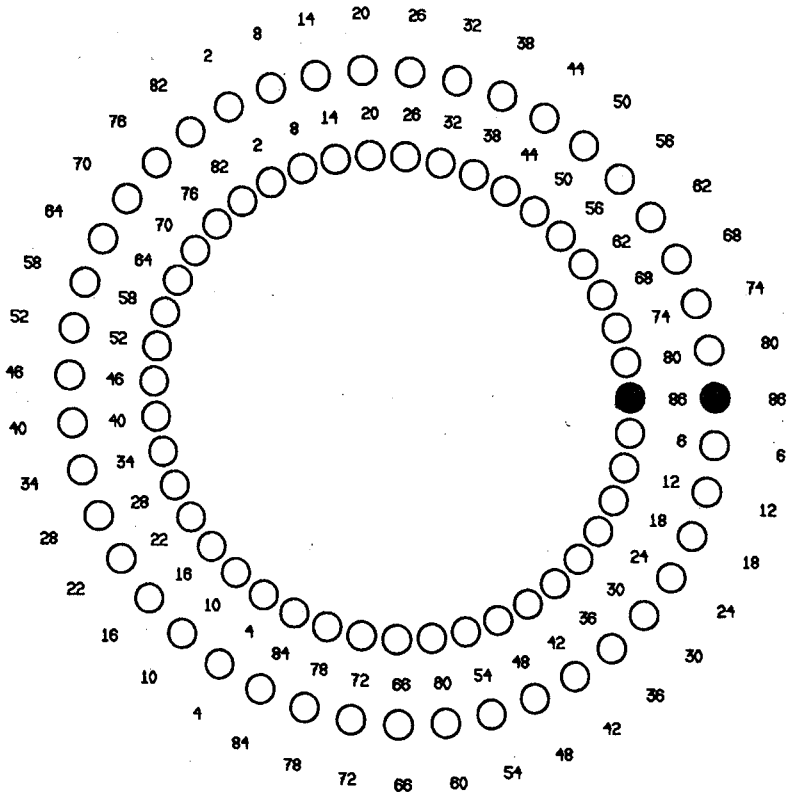

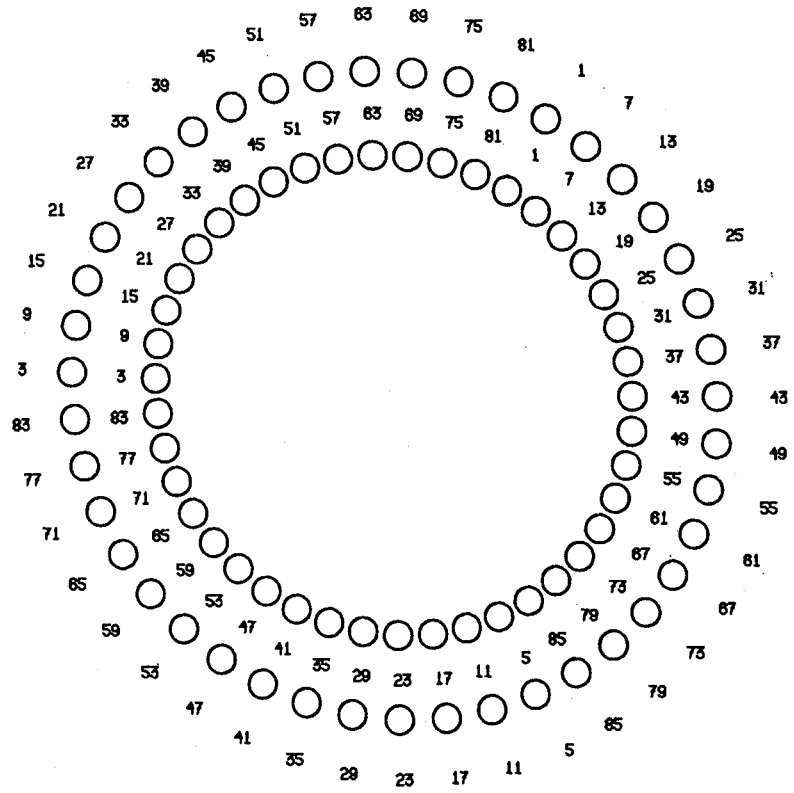

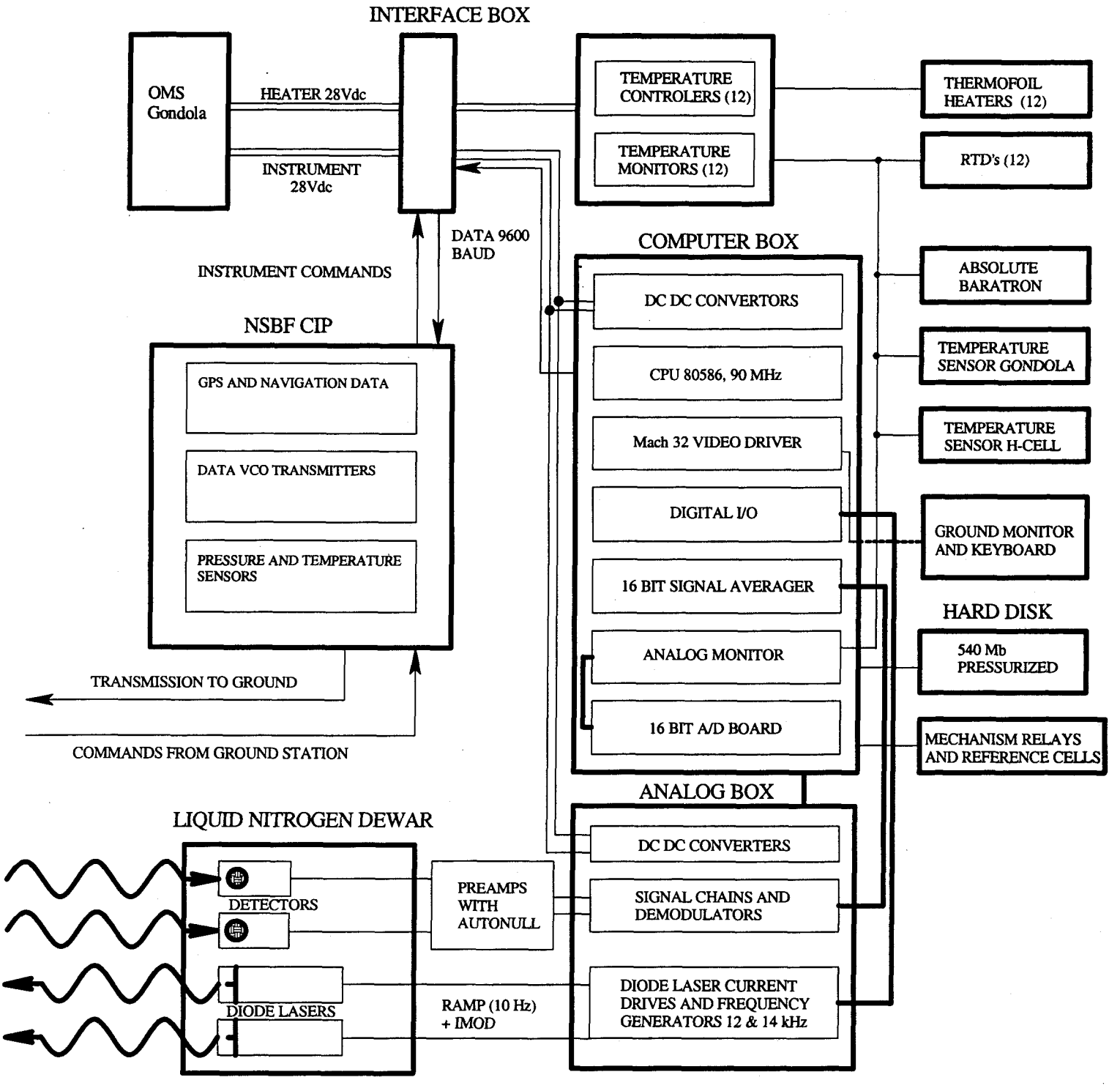
INTERFACE BOX
OMS Gondola
HEATER 28Vdc
INSTRUMENT 28Vdc
TEMPERATURE CONTROLERS (12)
TEMPERATURE MONITORS (12)
THERMOFOIL HEATERS (12)
RTD's (12)
DATA 9600 BAUD
INSTRUMENT COMMANDS
COMPUTER BOX
DC DC CONVERTORS
CPU 80586, 90 MHz
Mach 32 VIDEO DRIVER
DIGITAL I/O
16 BIT SIGNAL AVERAGER
ANALOG MONITOR
16 BIT A/D BOARD
ABSOLUTE BARATRON
TEMPERATURE SENSOR GONDOLA
TEMPERATURE SENSOR H-CELL
GROUND MONITOR AND KEYBOARD
HARD DISK
540 Mb PRESSURIZED
MECHANISM RELAYS AND REFERENCE CELLS
NSBF CIP
GPS AND NAVIGATION DATA
DATA VCO TRANSMITTERS
PRESSURE AND TEMPERATURE SENSORS
TRANSMISSION TO GROUND
COMMANDS FROM GROUND STATION
ANALOG BOX
DC DC CONVERTERS
SIGNAL CHAINS AND DEMODULATORS
DIODE LASER CURRENT DRIVES AND FREQUENCY GENERATORS 12 & 14 kHz
LIQUID NITROGEN DEWAR
DETECTORS
DIODE LASERS
PREAMPS WITH AUTONULL
RAMP (10 Hz) + IMOD

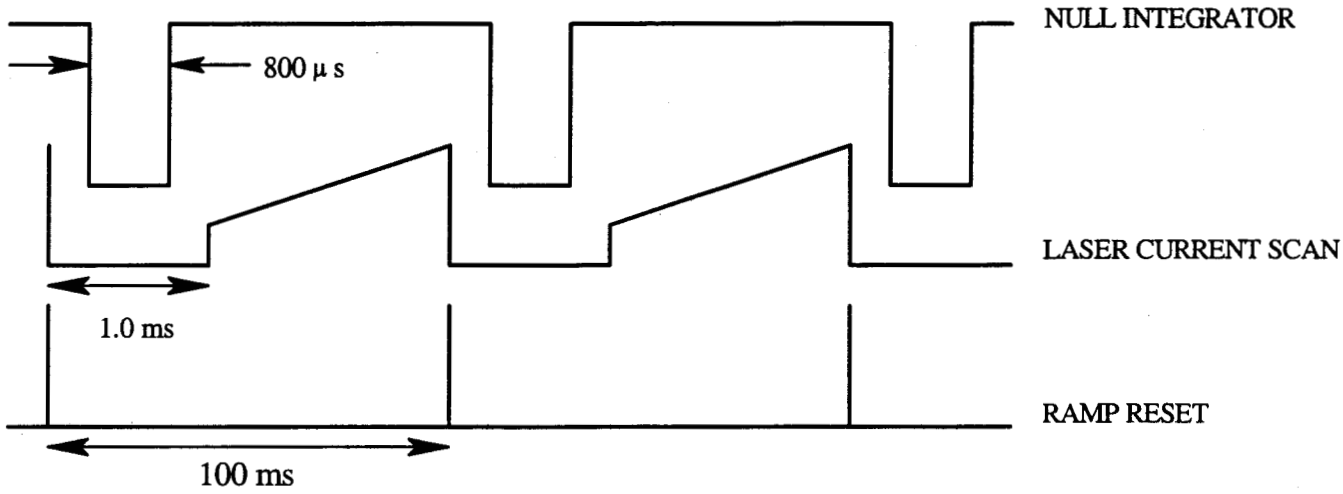

DOS FILE STRUCTURE

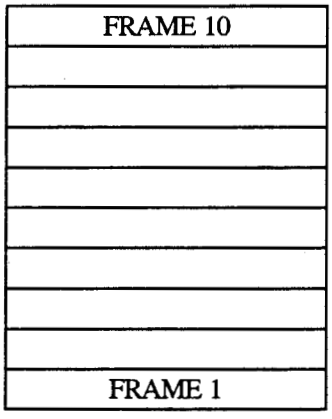

1 FRAME = 30 s
= 10 SUBFRAMES

DATA FRAME STRUCTURE

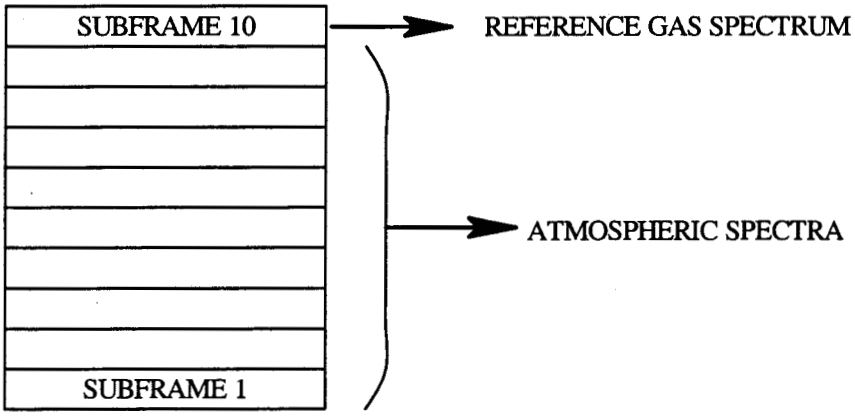

1 SUBFRAME = 3 s
= 30 scans

SUBFRAME STRUCTURE

AC1	AC2	DC1	DC2	HK

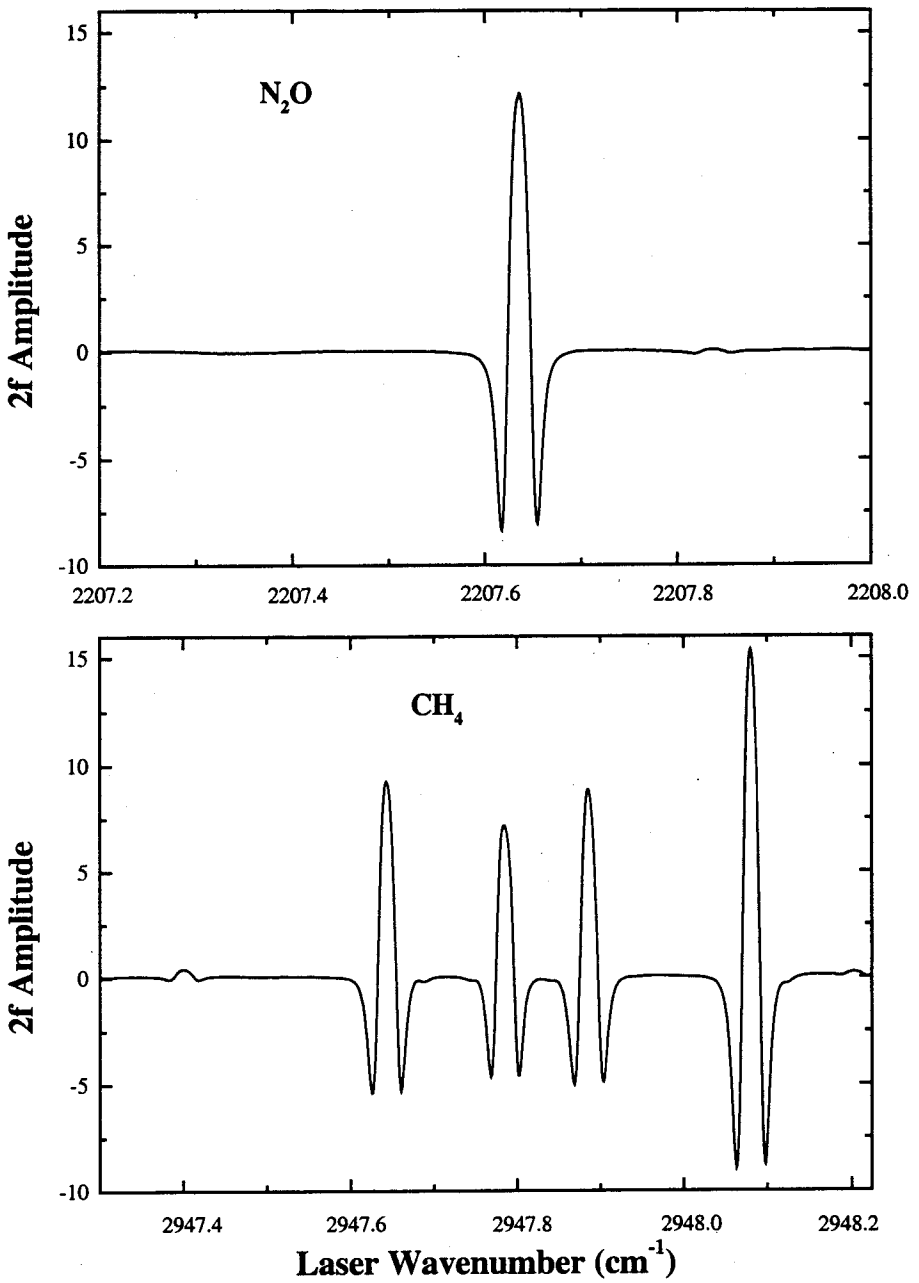
N2O
2f Amplitude
15
10
5
0
-5
-10
2207.2
2207.4
2207.6
2207.8
2208.0
CH4
2f Amplitude
15
10
5
0
-5
-10
2947.4
2947.6
2947.8
2948.0
2948.2
Laser Wavenumber (cm-1)

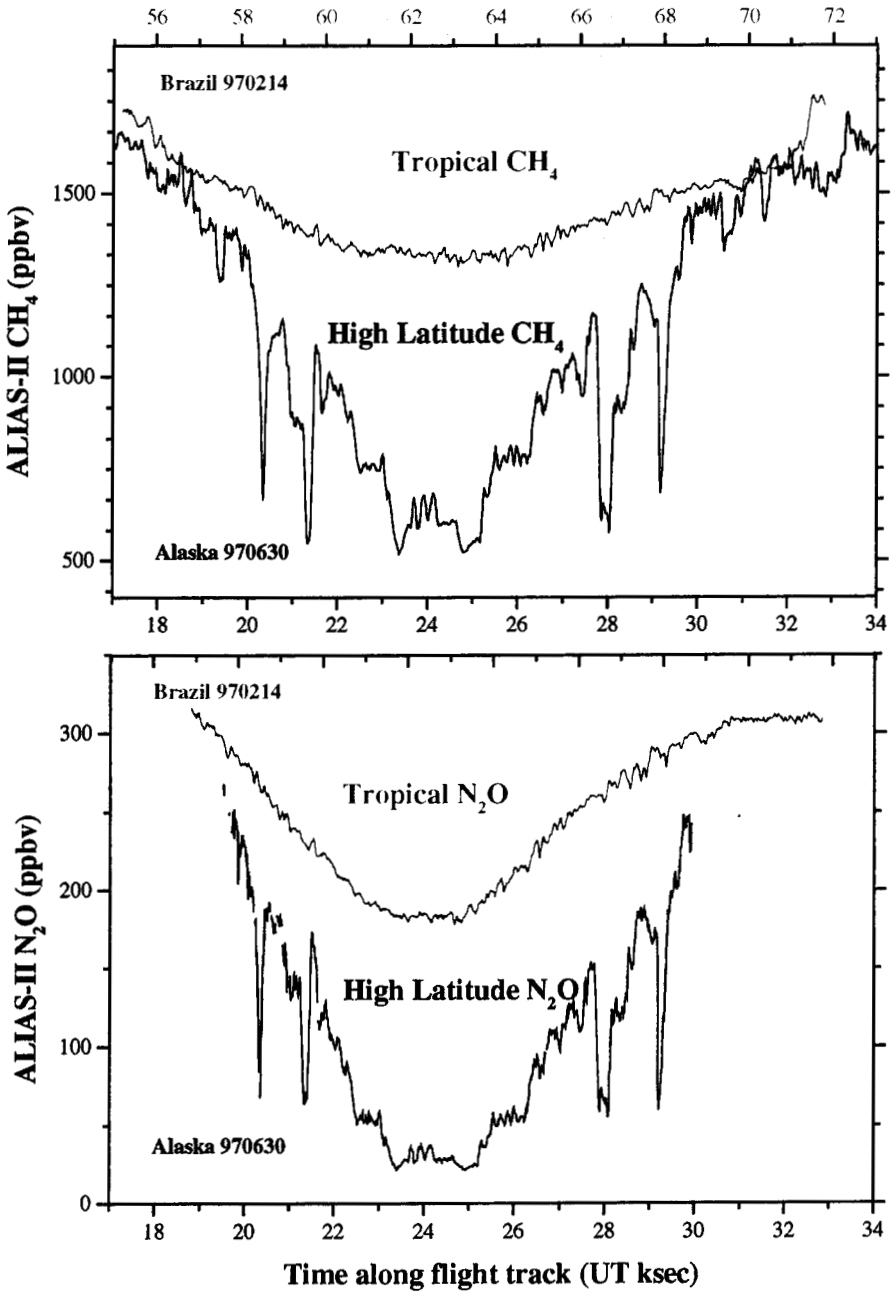
Brazil 970214
Tropical CH_4
High Latitude CH_4
Alaska 970630
ALIAS-II CH_4 (ppbv)
Brazil 970214
Tropical N_2O
High Latitude N_2O
Alaska 970630
ALIAS-II N_2O (ppbv)
Time along flight track (UT ksec)

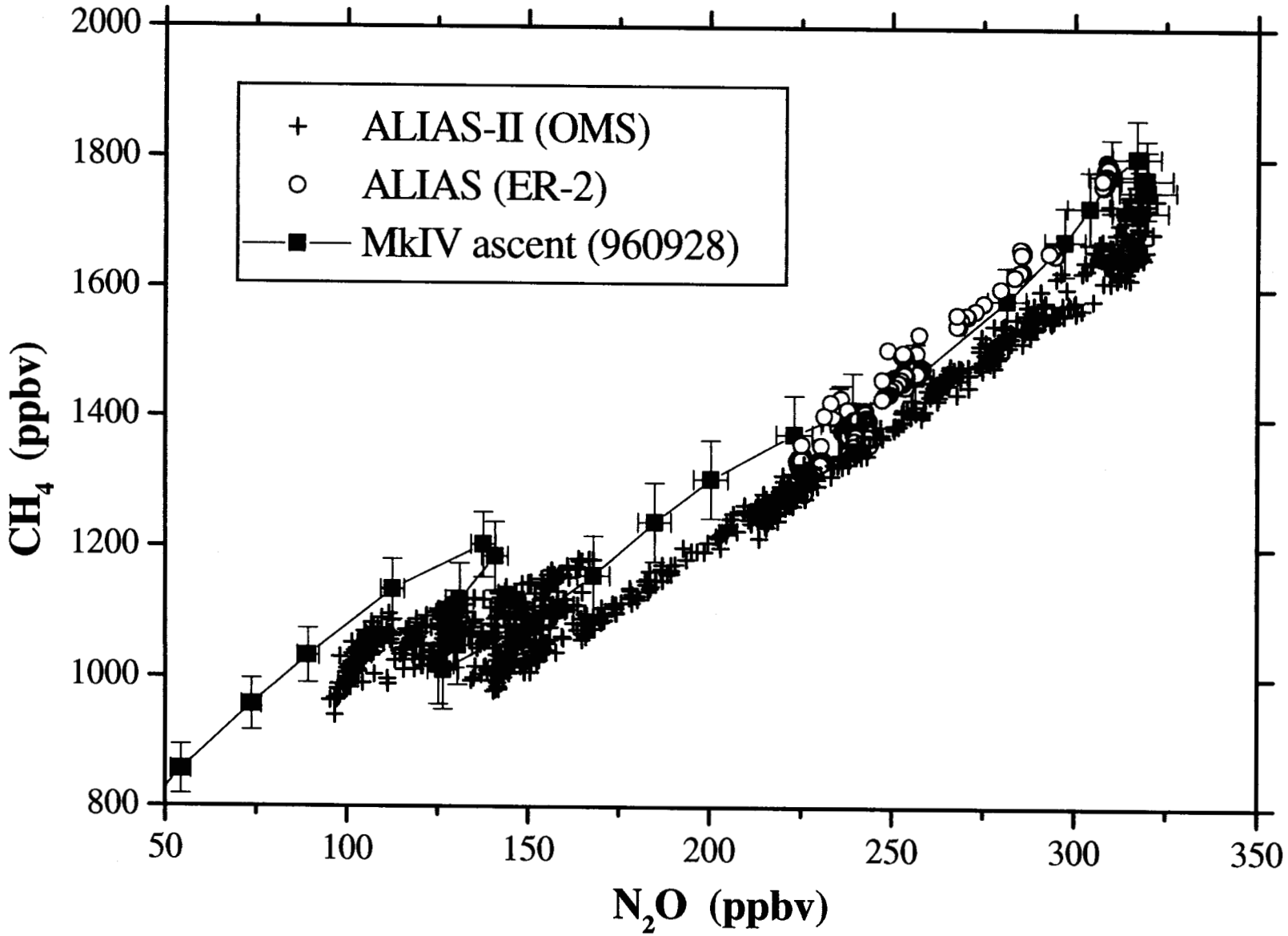
ALIAS-II (OMS)
ALIAS (ER-2)
MkIV ascent (960928)
CH4 (ppbv)
N2O (ppbv)
2000
1800
1600
1400
1200
1000
800
50
100
150
200
250
300
350

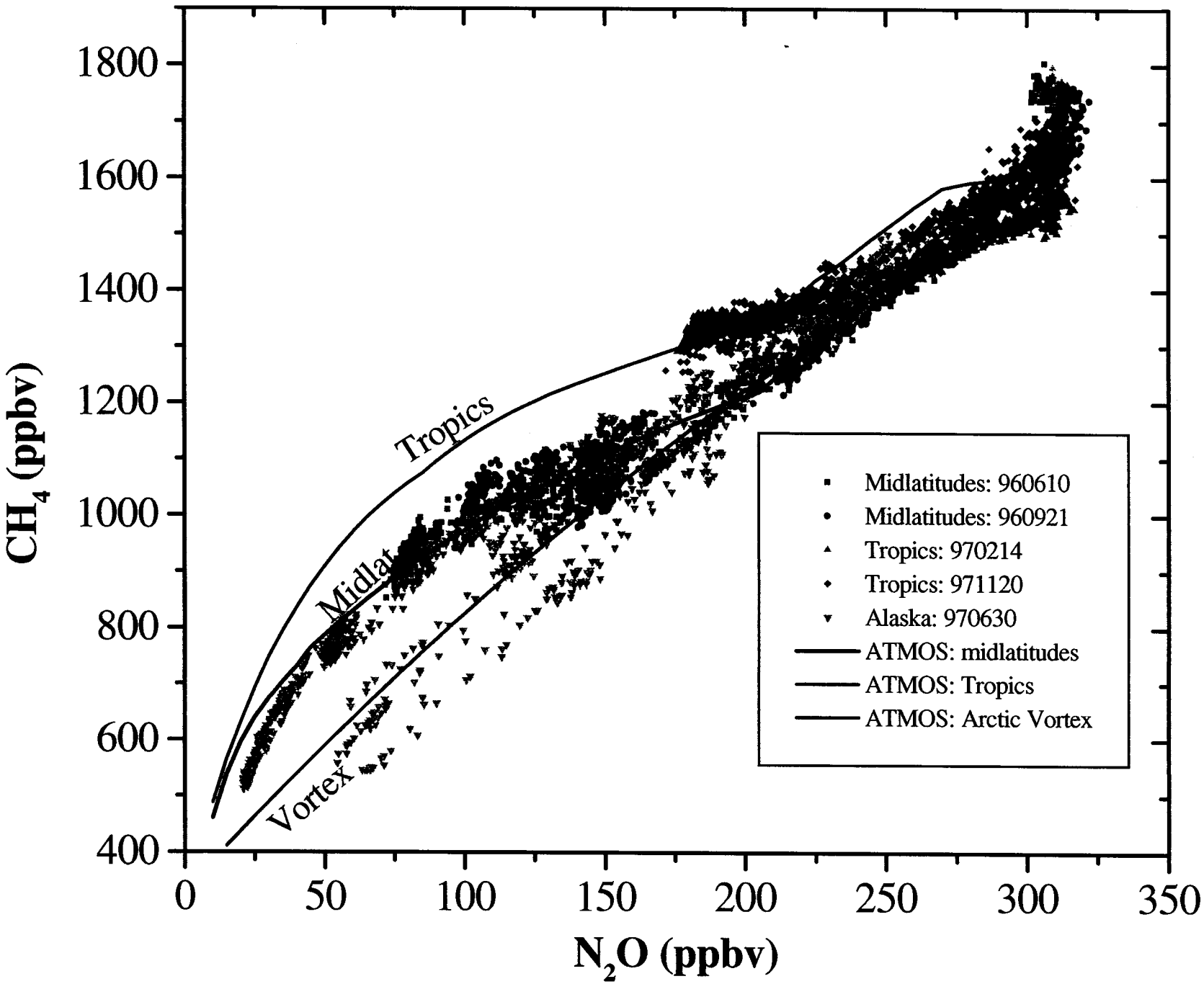
1800
1600
1400
1200
1000
800
600
400
0
50
100
150
200
250
300
350
CH_4 (ppbv)
N_2O (ppbv)
Tropics
Midlat
Vortex
Midlatitudes: 960610
Midlatitudes: 960921
Tropics: 970214
Tropics: 971120
Alaska: 970630
ATMOS: midlatitudes
ATMOS: Tropics
ATMOS: Arctic Vortex